



Contents lists available at ScienceDirect

Journal of Biomechanics

journal homepage: www.elsevier.com/locate/jbiomech

Replicating spine loading during functional and daily activities: An *in vivo*, *in silico*, *in vitro* research pipeline

I. Ebisch^a, D. Lazaro-Pacheco^a, D.J. Farris^b, T.P. Holsgrove^{a,*}^a Department of Engineering, Faculty of Environment, Science and Economy, University of Exeter, Exeter, UK^b Public Health & Sport Sciences, Faculty of Health and Life Sciences, University of Exeter, Exeter, UK

ARTICLE INFO

Keywords:

Spine biomechanics

Multi-axis

Intervertebral disc

Musculoskeletal modelling

*In silico**In vitro*

ABSTRACT

Lifestyle heavily influences intervertebral disc (IVD) loads, but measuring *in vivo* loads requires invasive methods, and the ability to apply these loads *in vitro* is limited. *In vivo* load data from instrumented vertebral body replacements is limited to patients that have had spinal fusion surgery, potentially resulting in different kinematics and loading patterns compared to a healthy population. Therefore, this study aimed to develop a pipeline for the non-invasive estimation of *in vivo* IVD loading, and the application of these loads *in vitro*. A full-body Opensim model was developed by adapting and combining two existing models. Kinetic data from healthy participants performing activities of daily living were used as inputs for simulations using static optimisation. After evaluating simulation results using *in vivo* data, the estimated six-axis physiological loads were applied to bovine tail specimens. The pipeline was then used to compare the kinematics resulting from the physiological load profiles (flexion, lateral bending, axial rotation) with a simplified pure moment protocol commonly used for *in vitro* studies. Comparing kinematics revealed that the *in vitro* physiological load protocol followed the same trends as the *in silico* and *in vivo* data. Furthermore, the physiological loads resulted in substantially different kinematics when compared to pure moment testing, particularly in flexion. Therefore, the use of the presented pipeline to estimate the complex loads of daily activities in different populations, and the application of those loads *in vitro* provides a novel capability to deepen our knowledge of spine biomechanics, IVD mechanobiology, and improve pre-clinical test methods.

1. Introduction

The degeneration of intervertebral discs (IVDs) has been linked to low back pain (Lotz and Chin, 2000), which is frequently encountered in clinical practice (Alzahrani et al., 2019). An increasing number of studies aim to replicate the *in vivo* environment in the *in vitro* setting to facilitate the investigation of IVD degeneration. Testing *in vitro* also provides a safe and replicable testing environment for the pre-clinical evaluation of new devices or regenerative treatments. However, the replication of complex six-axis physiological loads that the IVD is subjected to *in vivo* is hugely challenging. While there are an increasing number of research groups investigating spine biomechanics with six-axis test systems (Costi et al., 2021; Holsgrove et al., 2018), tests have generally been limited to stiffness matrix or pure moment tests, with or without the application of an axial preload. Replicating physiological loading during whole-organ IVD culture tests is also limited, with most

studies employing axial compression alone (Haglund et al., 2011; Illien-Jünger et al., 2010; Paul et al., 2012; Walter et al., 2011); though a small number of studies have applied sinusoidal rotations in axial rotation or bending in a single axis at a time, which may be combined with axial compression (Beatty et al., 2016; Chan et al., 2013; Hartman et al., 2015). These loading protocols do not account for the complex six-axis loading that the spine is subjected to during normal functional movements and daily activities, despite the studies that have been completed demonstrating that loading, and the type of loading applied, has a significant effect on IVD cell viability. This leads to a knowledge gap relating to the mechanobiology of the IVD and limits the effective pre-clinical evaluation of treatments and therapies for the IVD.

The lack of studies aiming to replicate the complex six-axis loads of the spine *in vivo* is likely due to both the technical challenge of controlling complex loading profiles in six-axis load control, along with limitations in the available input load data. While valuable data is

* Corresponding author at: Department of Engineering, Faculty of Environment, Science and Economy, University of Exeter, Harrison Building, North Park Rd, Exeter EX4 4QF, UK.

E-mail address: T.Holsgrove@exeter.ac.uk (T.P. Holsgrove).

<https://doi.org/10.1016/j.jbiomech.2023.111916>

Accepted 31 December 2023

Available online 5 January 2024

0021-9290/© 2024 The Author(s). Published by Elsevier Ltd. This is an open access article under the CC BY license (<http://creativecommons.org/licenses/by/4.0/>).

available from the Orthoload database (Bergmann, 2008), it is limited to patients that have undergone spinal fusion surgery so they may move differently to a healthy population. Computational musculoskeletal models and simulation methods provide a non-invasive alternative to estimate spinal loads in a range of populations and are becoming more popular for this purpose. The easily accessible, open-source musculoskeletal modelling platform OpenSim (Delp et al., 2007; Seth et al., 2018) provides a large database of models and standardised methods that have been developed and published by the research community, promoting opportunities for globally reproducible data.

Therefore, the aim of this study was to develop and test a pipeline which combines *in vivo*, *in silico*, and *in vitro* methods to allow the application of complex spinal loads from healthy participants to IVDs *in vitro*. Since simplified pure moment testing protocols have been widely used in previous studies of the spine, a further aim was to compare the kinematics resulting from applying six-axis load profiles with a simplified pure moment testing protocol.

2. Methods

2.1. Development of *in vivo*, *in silico*, *in vitro* pipeline

After obtaining approval by the institutional ethics committee (21-03-23-A-02), experimental data were collected from five healthy male participants without any recent history of back pain (age 27 ± 4 years; height 1.80 ± 0.80 m; mass 73 ± 9 kg). All participants were provided with an information sheet and provided written informed consent. The testing protocol included the collection of motion capture, ground reaction force (GRF) and surface electromyography (sEMG) data, with bi-polar electrodes on rectus abdominus, external obliques, lumbar longissimus and lumbar iliocostalis muscles in accordance with Seniam guidelines (SENIAM, 2022). These data were obtained for basic trunk movements: flexion with a straight back; flexion with a bent back; lateral bending; and axial rotation (Fig. 1S); as well as walking as an example of a daily activity with multi-axis loads. Participants performed the movements at a controlled, self selected pace. The pelvis was not

fixed, however participants were instructed to perform each movement within a range of motion (ROM) in which they did not have to move the pelvis. This ensured that movements were mainly performed through bending and twisting the spine, while a free pelvis allowed for a more natural movement than if it was fixed.

A musculoskeletal model for OpenSim (v4.3, SimTK, Stanford, CA) (Delp et al., 2007; Seth et al., 2018) was used to estimate lumbar load profiles. The full body model was adapted from the Lifting full body model, which had been validated for lifting tasks (Beaucage-Gauvreau et al., 2019), by adding bushing elements (Senteler et al., 2016) to all lumbar levels from S5/L1 to L1/T12 to represent passive joint stiffness. The values of the stiffness matrix for the bushing elements were not subsequently altered during the study. In addition, a thoracic ball joint was added to the trunk, allowing the model to simulate movements of the lumbar spine separately from the thoracic spine. This enabled the replication of physiological ROMs in the joints of the lumbar region from the *in vivo* input data. The generic model was scaled using OpenSim's Scaling Tool by calculating the ratio of the distance between experimental and virtual marker pairs for each body segment. To calculate spinal loads, motion capture and GRF data were used as inputs. SEMG data was used to evaluate muscle force estimates using static optimization (SO) (Fig. 1), and phase error (PE) and magnitude error (ME) were calculated for left and right erector spinae (Lund et al., 2011). In OpenSim, bushing moments and forces calculated with joint reaction analysis (JRA) are referenced about the centre of each joint. Therefore, simulated axial joint reaction forces (JRF) were compared with *in vivo* intradiscal pressure measurements without coordinate transformation, whereas the JRF at the two adjacent joints were averaged and transformed to the centre of the vertebral body to match the position of the coordinate system (COS) of the VBR.

The calculated axial compression forces for static poses of the *in silico* model for all five participants compared favourably with *in vivo* intradiscal pressure measurements normalised to standing (Takahashi et al., 2006; Wilke et al., 2001) and with absolute forces reported from *in vivo* studies (Schultz et al., 1982; Takahashi et al., 2006; Rohlmann et al., 2008) (Fig. 2S).

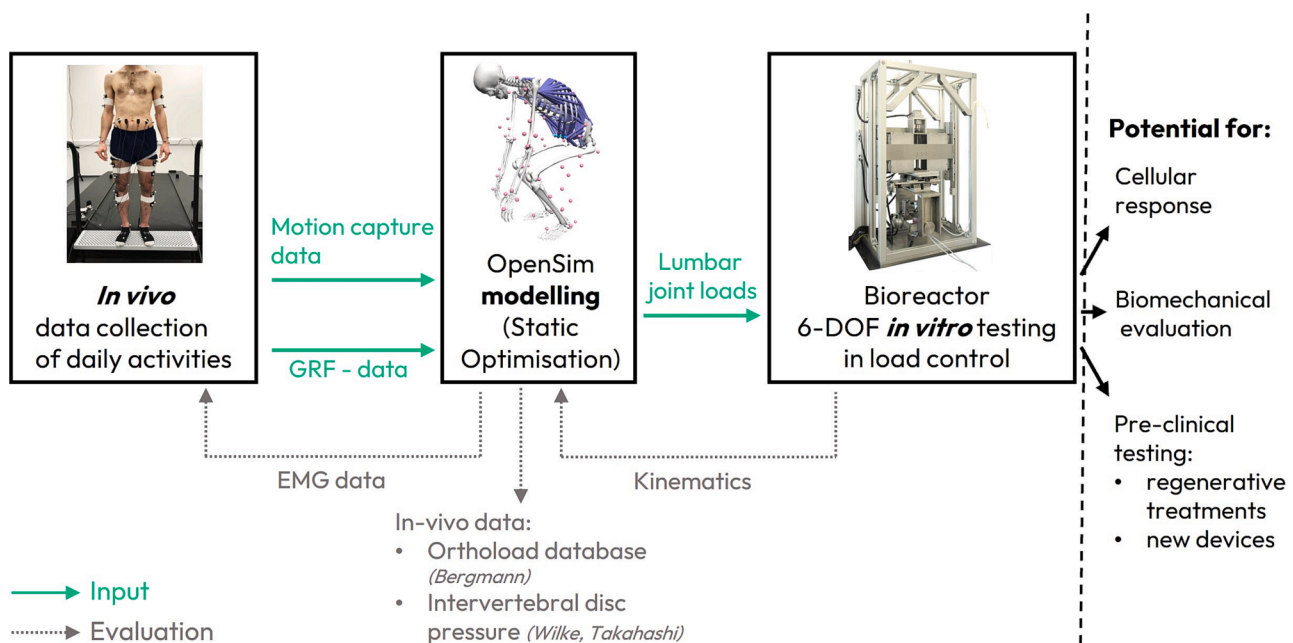


Fig. 1. By combining *in vivo*, *in silico* and *in vitro* methods, the research pipeline allows the estimation and application of complex lumbar IVD load profiles using kinematic and kinetic information from healthy participants. The outputs from *in vivo* data collection (motion capture data and GRF data) are used as inputs for the computational model to calculate spinal loads. The sEMG-data from *in vivo* data collection is used to evaluate muscle activation estimations of the computational model. The calculated spinal loads are the output of the *in-silico* part of this pipeline, and these loads are then used as input signals to operate a six-axis bioreactor in load control. To evaluate if the *in vitro* movement of the specimens corresponds to the *in silico* kinematics, kinematics of each primary axis are compared qualitatively.

For one participant (age 24 years; height 1.88 m; mass 71 kg), loads calculated at L1/L2 level were used as input signals for *in vitro* tests. The average sEMG errors for simulations with this in-silico model were 15.35 % and 13.7 % for PE and ME respectively in flexion, 5.9 % and 16.85 % for PE and ME respectively in right lateral bending, and 6.45 % and 7.6 % for PE and ME respectively in right axial rotation.

The six-axis loads were used as input signals to operate a six-axis bioreactor in load control, which was based on a previously developed six-axis spine simulator (Holsgrove et al., 2017). The loads were applied to the centre of the superior vertebral body and the spine simulator was updated to include a test chamber to maintain specimens in a fluid bath.

2.2. Application and evaluation of physiological load profiles for *in vitro* tests

The pipeline was used to investigate the effects of applying physiological six-axis loads estimated from healthy participants to IVDs *in vitro* and compare resulting kinematics from this novel pipeline with those from a pure bending moment protocol. To investigate the effects of the different loading protocols on specimen kinematics, three load cases were developed for the following movements: flexion with a straight back, flexion with a bent back; lateral bending to the right; and axial rotation to the right. The three load cases increased in complexity from pure moments through to the replication of complex six-axis load profiles (Fig. 2):

Pure moment sine wave protocol (case 1).

A sine wave was applied in the primary axis in positive and negative directions, and a constant preload equal to the *in silico* estimate during relaxed standing was applied in axial compression. All other axes (shear forces, and non-primary rotational axes) were maintained at 0 N, and

0 Nm (Fig. 2, a, d).

Physiological pure moment protocol (case 2).

Model estimates of joint load profiles were used to apply a moment in the primary rotational axis and the axial compression force. All other axes were maintained at 0 N, and 0 Nm (Fig. 2, b, e).

Six-axis physiological loading protocol (case 3).

Model estimates were used to apply moments and forces in all six axes (Fig. 2, c, f).

To evaluate the capability of the pipeline to be applied to complex activities with multi-axis loads, *in silico* load estimates from the same participant of walking two steps were used as an example of a daily activity.

All test cases were completed in six-axis load control using bovine tail specimens. To account for the smaller size of bovine tail IVDs, magnitudes of all loads from the model were scaled down by a factor of four, which is an average of the ratio of the cross-sectional area of a human IVD (1950 mm²) (Beckstein et al., 2008) with respect to bovine tails used in this study. Furthermore, to avoid unwanted oscillations due to the challenges of applying six-axis load control to spinal specimens, all load signals were slowed down by a factor of 10 (Lazaro-Pacheco and Holsgrove, 2023).

Bovine tails were acquired on the day of slaughter from the local abattoir with skin already removed. Tails were dissected to provide vertebra-IVD-vertebra specimens (n = 5) of the first two coccygeal IVDs (Cx1-2 and Cx2-3). Soft tissue was removed using a scalpel and scissors, and processes were cut using an oscillating bone saw. Following removal of soft tissue and processes, the cranial and caudal vertebrae of each level were cut in the transverse plane, leaving approx. 15 mm of bone on

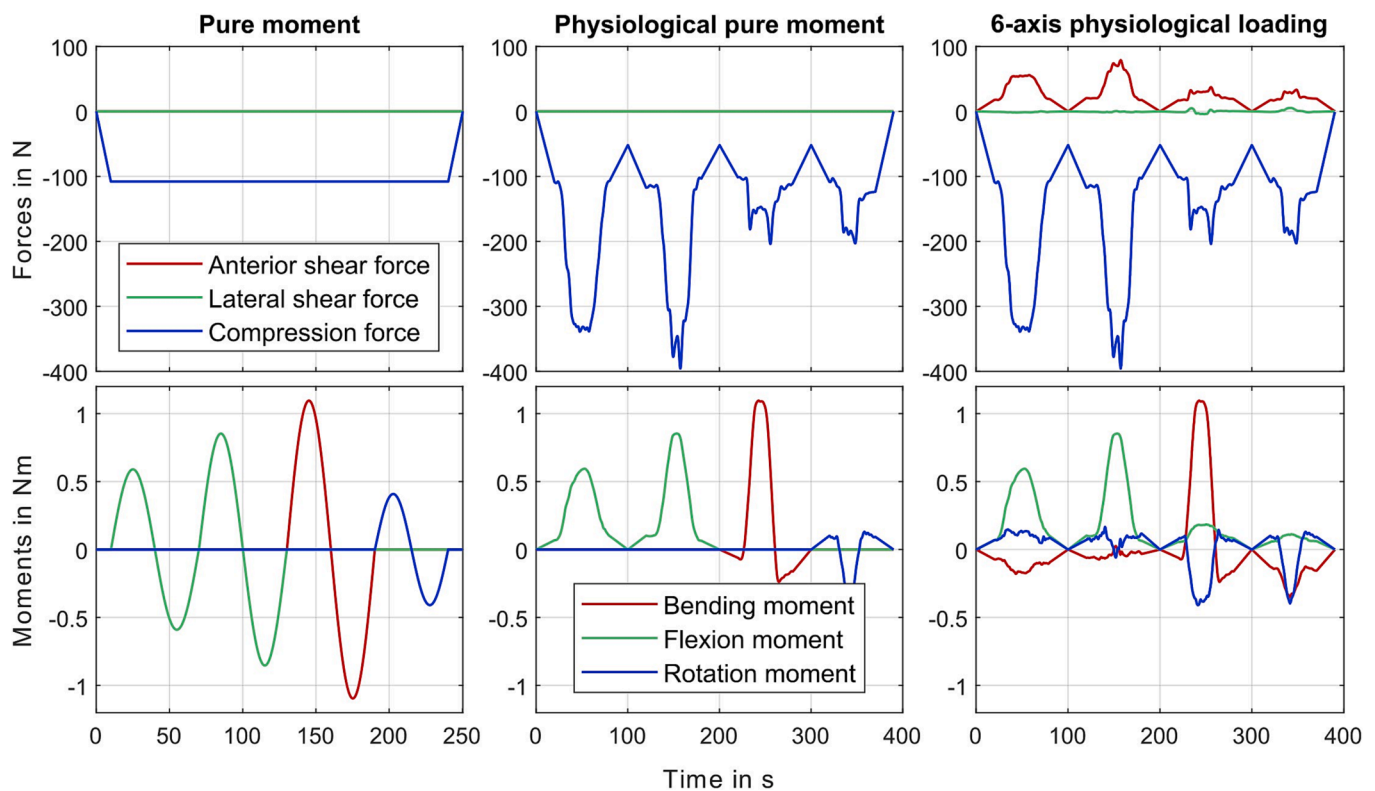


Fig. 2. Input signals for six-axis load control in the three cases. Load profiles included loads from movements in the following sequence: flexion with a straight back, flexion with a bent back, lateral bending to the right, and axial rotation to the right. Starting from 0 N/Nm demand, a 10 s ramp was used to reach each starting value. Between movements, axial compression was 52 N to maintain the specimen in a stable upright position and it also replicated the minimum compression the IVD subjected to due to muscle and ligament tension.

each side of the IVD. During dissection the following measurements were taken using a digital calliper: anterior-posterior and lateral diameter of the IVD; the distance from the cranial cut to the centre of the caudal vertebra, and the overall height of the specimen. Following dissection, specimens were wrapped in Phosphate-buffered saline (PBS)-soaked tissue paper and stored in sealed plastic bags at -20°C until the day of testing, when specimens were removed from the freezer and thawed at room temperature.

On the day of testing, specimens were placed and mounted in the biochamber with the cranial vertebra at the bottom, to be equivalent to the human lumbar spine with the larger vertebra of a motion segment located caudally of the IVD. The biochamber was filled with PBS until the specimen was fully submerged and then sealed. The filled chamber was then transferred to the six-axis test system, placed on the load cell (HBM MCS10), and the load was zeroed to account for the weight of the filled chamber. The biochamber was then rigidly mounted into the test system. Once the biochamber was mounted, the translations and rotations of all six axes were manually adjusted to return the load to zero, and the position was then zeroed to provide the test neutral position. Following this initial set-up, a preload of 108 N, equivalent to the force calculated by the model in a relaxed standing position was applied before each test for a period of 1 h to equilibrate the specimen. Using the height measurements taken during dissection, loads were transformed in real-time from the load cell datum below the specimen, to the centre of the upper vertebra. Following the equilibration period, the functional movements were applied to all specimens in the order presented in Fig. 2, followed by the loads representing walking (Fig. 6). To investigate the effects of increasing complexity on specimen kinematics, both rotations and translations were evaluated for flexion with a bent spine, lateral bending to the right and axial rotation to the right for $n = 5$

specimens (Figs. 3-5). In addition to the comparison of kinematics between load cases, the kinematics of the primary axes during each *in vitro* test (e.g., flexion during the flexion tests) were compared with the segmental kinematics of the *in silico* model.

3. Results

In flexion, the pure moment sine wave protocol (case 1) led to a peak flexion angle of $7.0 \pm 3.3^{\circ}$, which was closest to the *in silico* model peak ROM of 8.4° (Table 1). The physiological pure moment (case 2), and six-axis physiological loading (case 3) protocols led to peak flexion angles of $2.0 \pm 0.4^{\circ}$ and $2.3 \pm 0.5^{\circ}$, respectively. The non-primary rotational axes did not vary substantially from zero (Fig. 3, bottom row). However, the translations differed substantially, with axial translation increasing in case 1, meaning that the IVD height increased during flexion, which did not occur when a physiological axial compression was applied in cases 2 and 3 (Fig. 3, top row). Furthermore, the anterior-posterior translation was also negative during load cases 1 and 2, meaning the superior vertebra moved posteriorly during flexion, but not in load case 3, when the six-axis physiological load profile included an anterior shear force.

In lateral bending, the kinematics showed similar trends across all load cases with peak ROM ranging from $9.8 \pm 1.3^{\circ}$ for case 1 to $8.0 \pm 1.0^{\circ}$ and $8.0 \pm 0.9^{\circ}$ for cases 2 and 3 respectively (Fig. 4, bottom row). The peak ROM of all cases were greater than the model results of 4.3° (Table 1). The non-primary rotational axes remained close to zero in cases 1 and 2, however the additional axial rotation moment of case 3 resulted in an axial rotation to the right of $2.0 \pm 1.0^{\circ}$ during lateral bending to the right (Fig. 4, f). All load cases also exhibited similar translational behaviour, with a decrease in IVD height during lateral bending, combined with a lateral movement of the superior vertebral

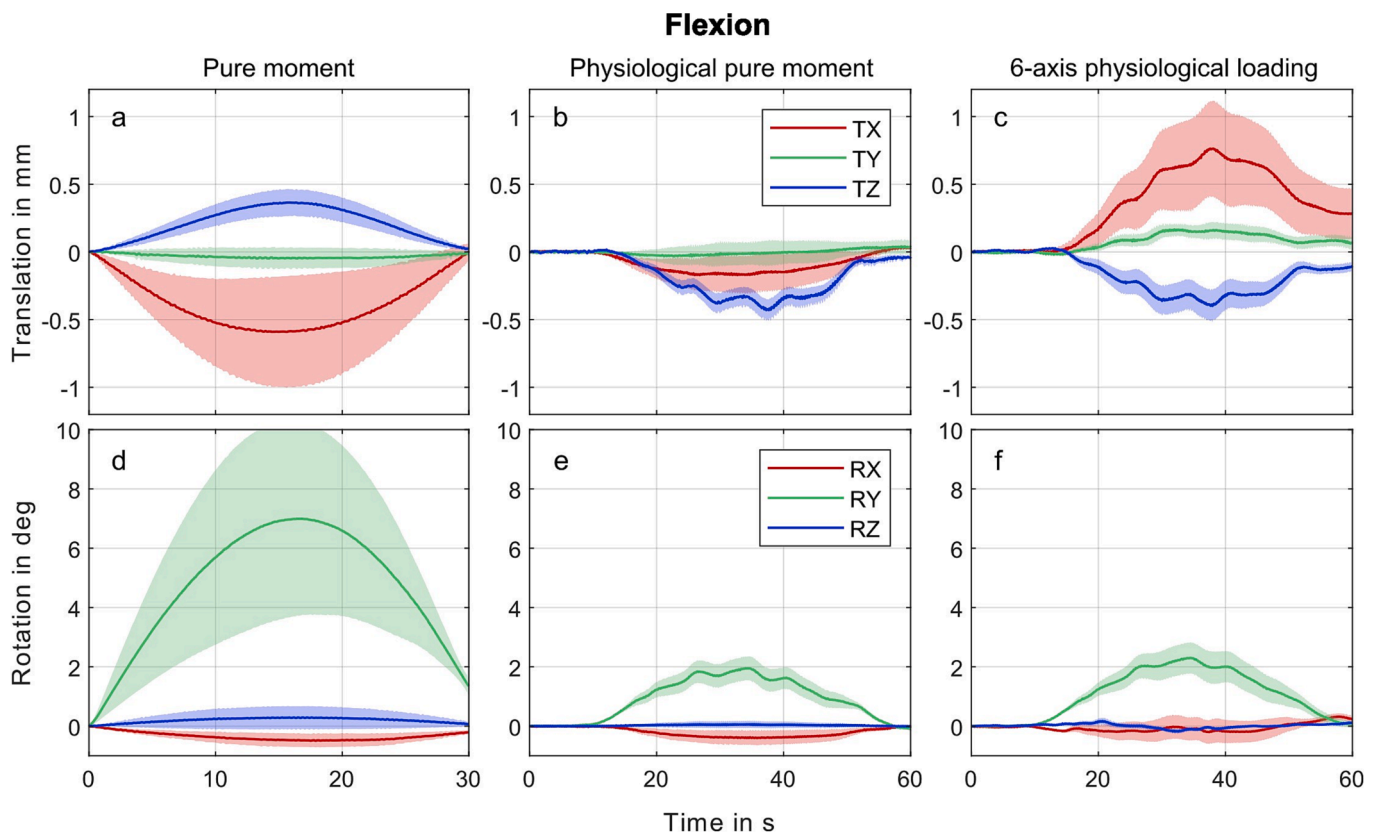


Fig. 3. *In vitro* kinematics of $n = 5$ specimens during flexion with a bent back with: anterior translation, TX; left lateral translation, TY; cranial translation, TZ; right lateral bending, RX; flexion, RY; and left axial rotation, RZ. Translations (top row) and rotations (bottom row) for the three load cases: pure moment sine wave protocol (left column); physiological pure moment protocol (centre column); and six-axis physiological loading protocol (right column). Mean and standard deviation kinematics are shown as a line and shaded area respectively for each axis.

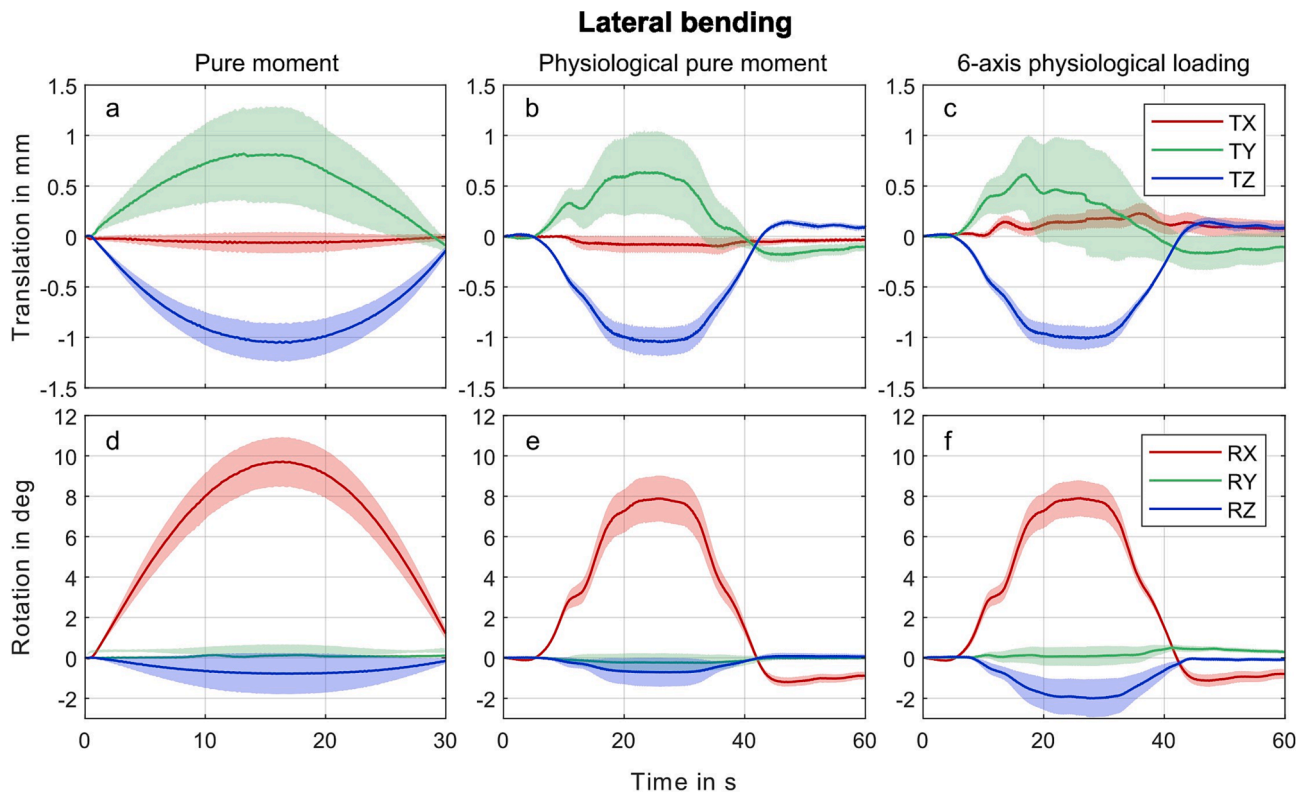


Fig. 4. *In vitro* kinematics of $n = 5$ specimens during lateral bending to the right side with: anterior translation, TX; left lateral translation, TY; cranial translation, TZ; right lateral bending, RX; flexion, RY; and left axial rotation, RZ. Translations (top row) and rotations (bottom row) for the three load cases: pure moment sine wave protocol (left column); physiological pure moment protocol (centre column); and six-axis physiological loading protocol (right column). Mean and standard deviation kinematics are shown as a line and shaded area respectively for each axis.

body to the right (Fig. 4, top row).

With peak ROM for the primary axis of $0.8 \pm 0.3^\circ$ and $0.7 \pm 0.3^\circ$, cases 2 and 3 reached similar peak ROM during axial rotation to the right (Fig. 5, e, f) to that from the model of 0.6° (Table 1) while case 1 presented the largest ROM with $1.2 \pm 0.3^\circ$. In load cases 1 and 2 the non-primary rotational axes were maintained close to zero during testing (Fig. 3), but in load case 3 the axial rotation was combined with lateral bending to the opposite side and a small amount of flexion (Fig. 3). For all three load cases the translations were generally lower than 0.15 mm, with the biggest difference found in axial translations, in which load cases 1 and 2 resulted in a small decrease in IVD height (Fig. 5, a, b), whereas no notable change in IVD height was observed in load case 3 (Fig. 5, c).

Measured forces and moments during the *in vitro* testing for walking two steps closely matched the desired loads (Fig. 6), demonstrating that the *in vivo*, *in silico*, *in vitro* pipeline can be employed to replicate complex daily activities involving multi-axis loads, in addition to the functional movements of flexion, lateral bending, and axial rotation that are more limited to a primary axis.

4. Discussion

Using the presented pipeline, complex six-axis lumbar load profiles were successfully applied to bovine IVDs *in vitro*. Because measuring spinal loads *in vivo* is only possible through highly invasive methods, six-axis data that can be used as input for spinal testing is limited to patients that have undergone spinal fusion surgery (Rohmann et al., 2008). The current paper has shown the feasibility of addressing this limitation through the presented *in vivo*, *in silico*, *in vitro* pipeline, which employs musculoskeletal modelling to estimate spinal loading. Our approach can therefore be applied to different population groups in the future.

4.1. Comparison of kinematics from three load cases

Comparing the kinematics from all three load cases for basic trunk movements revealed substantial differences that arise from applying a physiological six-axis load profile as opposed to applying simplified protocols using a pure moment in a single axis combined with a constant axial preload, which is commonly used for *in vitro* studies (Costi et al., 2021). In particular, cases 1 and 3 for trunk flexion (Fig. 3) resulted in fundamentally different movement patterns, while differences were less pronounced for lateral bending and axial rotation. Considering that the working population spends most of the day sitting in a slightly flexed posture (Bauman et al., 2011), there is a need to provide physiological loading patterns for *in vitro* IVD testing protocols. Previous pure moment tests with a fixed TZ axis showed an increase in axial compression during flexion (Holsgrove et al., 2017), similar to results obtained during intradiscal pressure measurements (Wilke et al., 2001). These findings emphasise that the increased axial compression applied during flexion in cases 2 and 3 is more physiological than using the constant compression force of case 1, which led to an increase in IVD height (Fig. 3, a). The difference in peak ROM of approximately 6° for flexion between case 1, and cases 2 and 3 suggest that the magnitude of axial compression greatly influenced the stiffness of the IVD. These findings are in line with previous studies highlighting an increase in IVD stiffness due to axial preload (Holsgrove et al., 2015; Stokes and Gardner-Morse, 2003). The magnitude of preload used while applying bending moments must therefore be critically assessed in future studies as well as when comparing results between studies. Differences in peak ROM between *in vitro* and *in silico* results can likely be attributed to the large neutral zone of bovine IVDs, especially in lateral bending. However, the biochemical composition, cell density and the type of cells of bovine IVDs are highly similar to human IVDs (Gantenbein et al., 2015). These similarities and the easy accessibility of bovine specimens as part of the human food

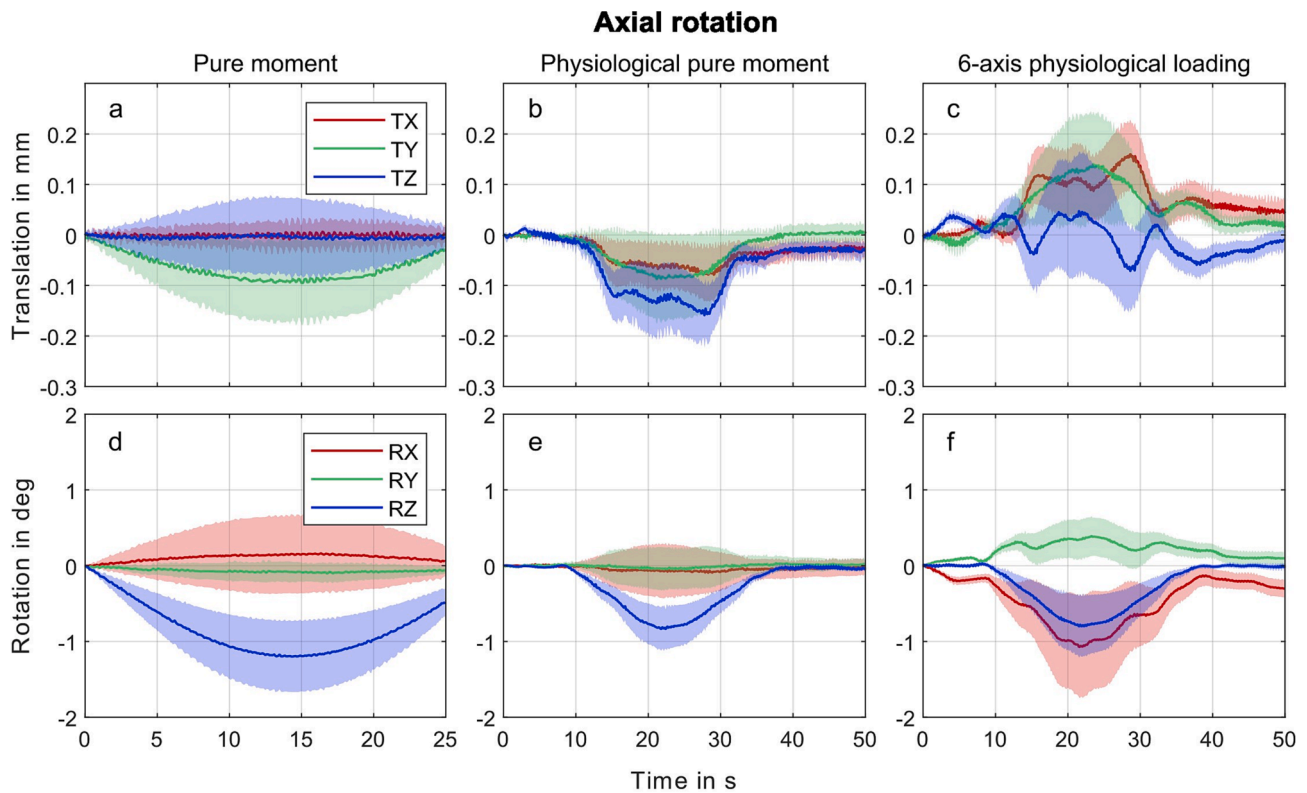


Fig. 5. *In vitro* kinematics of $n = 5$ specimens during axial rotation to the right side with: anterior translation, TX; left lateral translation, TY; cranial translation, TZ; right lateral bending, RX; flexion, RY; and left axial rotation, RZ. Translations (top row) and rotations (bottom row) for the three load cases: pure moment sine wave protocol (left column); physiological pure moment protocol (centre column); and six-axis physiological loading protocol (right column). Mean and standard deviation kinematics are shown as a line and shaded area respectively for each axis.

chain make it an attractive model that has been used in numerous previous *in vitro* studies (Beatty et al., 2016; Chan et al., 2013; Gawri et al., 2014; Haglund et al., 2011; Walter et al., 2011).

Kinematics determined from *in vivo* experimental data collection reveal that small secondary rotations exist for most movements performed by participants from this study. Neglecting these off-axis moments in load cases 1 and 2 led to qualitative differences in kinematics, especially in axial rotation (Fig. 5, bottom row). Confirming the relevance of these findings, lateral bending during axial rotation was also observed during an MRI-study (Fujii et al., 2007) and load case 3 best replicated the *in silico* kinematics, with left lateral bending occurring during right axial rotation (Fig. 5, f). Using walking as an example of an activity including bending and twisting of the spine simultaneously, we were able to demonstrate the capability of the pipeline to be applied to complex activities of daily living (Fig. 6). Given that the load cases presented qualitative differences in *in vitro* kinematics for the simplified functional movements included in this study, we conclude that daily activities might only be reasonably replicated *in vitro* using six-axis test protocols.

4.2. Limitations

One limitation of the current pipeline is that *in vivo* kinematics obtained with skin-mounted motion capture markers cannot provide the necessary accuracy to track both rotations and translations of the vertebrae. Additionally, although the bushings used to simulate passive joint stiffness in the computational model did include translational DOF and would allow for a moving centre of rotation (COR) (Senteler et al., 2016), all lumbar joints were constrained to three rotational DOF. To address this limitation in the future, the current *in vivo* experimental setup could be combined with biplanar X-ray fluoroscopy to track bone motion more directly. The combination of these techniques would allow

more precise estimation of segmental motion, while obtaining kinematic information of the whole body from the motion capture data. These data could be used either as input for the computational model to estimate loads, or the kinematics might be applied directly to IVDs *in vitro*. However, this method would have limitations due to the ionising radiation of the fluoroscopy and the field of view of the biplanar test set-up, which may limit the duration and types of activities that can be captured.

Furthermore, SO, which is currently used to solve the muscle redundancy problem may be substituted in the future with a more advanced method, such as the incorporation of EMG-informed optimisations and direct collocation approaches to improve the accuracy of spinal load calculation.

To operate the test system in six-axis load control, signals had to be slowed down (Lazaro-Pacheco and Holsgrove, 2023). A comparison of frequency dependent behaviour (4 tested frequencies of 0.001, 0.01, 0.1, and 1 Hz) showed that the overall increase in stiffness over the 4 decades was 35 %, 33 %, and 26 % for anterior-posterior shear force, lateral shear force, and axial rotation respectively, and 45 %, 29 %, 51 %, and for compression, lateral bending, flexion (Costi et al., 2008). Therefore, small differences in stiffness between the original and slowed down speeds may have been introduced, however the differences observed between cases analysed in this study should not have been influenced substantially, as they were all completed at the same test rate.

5. Conclusions

The presented research pipeline allows the application of complex lumbar spinal load profiles from healthy participants on a six-axis test system by combining *in vivo*, *in silico* and *in vitro* methods. The application of calculated loads from healthy participants to IVDs *in vitro* completed in this study has not previously been achieved and provides

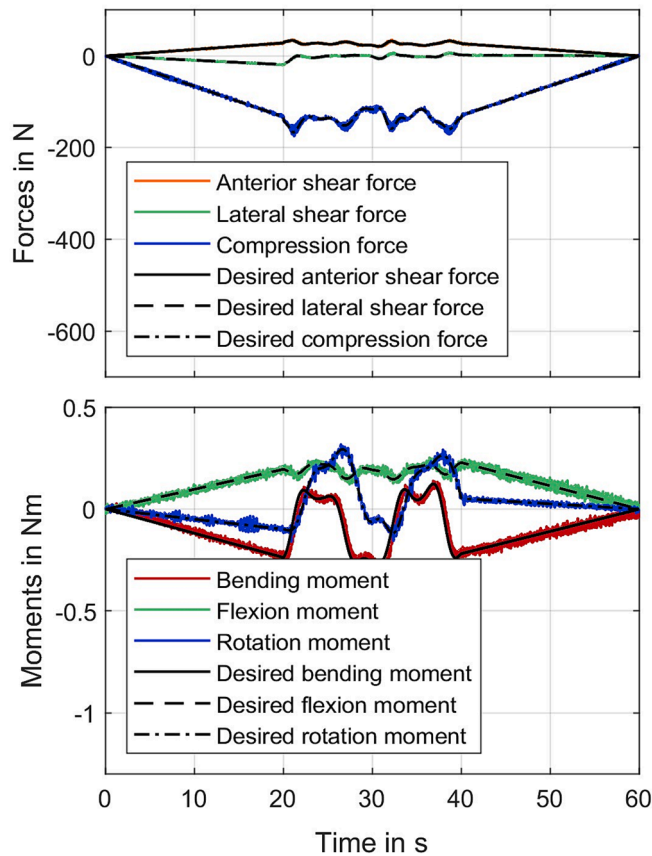


Fig. 6. Measured loads to replicate the complex loading in multiple axes during walking were calculated from the *in vivo* data and *in silico* model, and were then slowed down and scaled to the cross-sectional area of a bovine tail specimen. These loads were then used as the input signals using the six-axis test system in load control to demonstrate the capability of the system to closely match complex loads that go beyond idealised movements. Typical desired and actual load data for a single bovine tail specimen is shown. Two 2 s ramps were used at the beginning and end of the load signals to provide a smooth transition from 0 N/Nm to the first value of the calculated loads to avoid a step change in load signal that might lead to oscillations during *in vitro* testing.

Table 1

In vitro peak ROMs of each primary axis of all three test protocols were compared with the *in silico* kinematics. This allows a comparison of peak ROMs using the different *in vitro* loading protocols with each other, and with the *in silico* model used to drive them. *In silico* ROMs were derived from the *in vivo* motion capture data.

Test protocol	Peak ROM primary axis (°)		
	Flexion (RY)	Lateral bending (RX)	Axial rotation (RZ)
Case 1 (Pure moment sine wave & constant axial compression)	7.0 ± 3.3°	9.8 ± 1.3°	1.2 ± 0.5°
Case 2 (Pure moment & estimated axial compression)	2.0 ± 0.4°	8.0 ± 1.0°	0.8 ± 0.3°
Case 3 (Six-axis load profile)	2.3 ± 0.5°	8.0 ± 0.9°	0.7 ± 0.3°
<i>In silico</i> model	8.4°	4.3°	0.6°

evidence that the pipeline can be used effectively, providing a state-of-the-art research pipeline with which to estimate and replicate complex spinal loads. Because the pipeline uses non-invasive methods to estimate spinal load profiles, it offers the potential to expand currently available load profiles to specific population groups to provide a greater understanding about population-level and individual spine biomechanics. The load profiles might also be adopted in whole organ IVD culture models,

providing the capability to deepen our knowledge of how mechanical and biochemical environments interact. Such tests also have the potential to improve *in vitro* evaluation of new treatments such as regenerative therapies or IVD replacements.

CRedit authorship contribution statement

I. Ebisch: Conceptualization, Data curation, Writing – original draft, Writing – review & editing, Visualization, Investigation, Validation, Formal analysis, Methodology, Software. **D. Lazaro-Pacheco:** Data curation, Writing – review & editing, Investigation, Methodology, Supervision, Software. **D.J. Farris:** Conceptualization, Writing – review & editing, Methodology, Supervision, Resources. **T.P. Holsgrove:** Conceptualization, Funding acquisition, Writing – review & editing, Methodology, Supervision, Resources, Project administration.

Declaration of competing interest

The authors declare that they have no known competing financial interests or personal relationships that could have appeared to influence the work reported in this paper.

Acknowledgements

The authors would like to acknowledge the EPSRC training grant (EP/T518049/1 #2606307) and the EPSRC research grant (EP/S031669/1), which supported the completion of this research.

Appendix A. Supplementary data

Supplementary data to this article can be found online at <https://doi.org/10.1016/j.jbiomech.2023.111916>.

References

Alzahrani, H., Shirley, D., Cheng, S.W.M., Mackey, M., Stamatakis, E., 2019. Physical activity and chronic back conditions: A population-based pooled study of 60,134 adults. *J. Sport Health Sci.* 8, 386–393. <https://doi.org/10.1016/j.jshs.2019.01.003>.

Bauman, A., Ainsworth, B.E., Sallis, J.F., Hagströmer, M., Craig, C.L., Bull, F.C., Pratt, M., Venugopal, K., Chau, J., Sjöström, M., 2011. The descriptive epidemiology of sitting: A 20-country comparison using the international physical activity questionnaire (IPAQ). *Am. J. Prev. Med.* 41, 228–235. <https://doi.org/10.1016/j.amepre.2011.05.003>.

Beatty, A.M., Bowden, A.E., Bridgewater, L.C., 2016. Functional Validation of a Complex Loading Whole Spinal Segment Bioreactor Design. *J. Biomech. Eng.* 138, 64501–65011. <https://doi.org/10.1115/1.4033546>.

Beaucage-Gauvreau, E., Robertson, W.S.P., Brandon, S.C.E., Fraser, R., Freeman, B.J.C., Graham, R.B., Thewlis, D., Jones, C.F., 2019. Validation of an OpenSim full-body model with detailed lumbar spine for estimating lower lumbar spine loads during symmetric and asymmetric lifting tasks. *Comput. Methods Biomech. Biomed. Eng.* 22, 451–464. <https://doi.org/10.1080/10255842.2018.1564819>.

Beckstein, J.C., Sen, S., Schaefer, T.P., Vresilovic, E.J., Elliott, D.M., 2008. Comparison of Animal Discs Used in Disc Research to Human Lumbar Disc Axial Compression Mechanics and Glycosaminoglycan Content. *Spine* 33, E166–E173.

Bergmann, G. e., Charité – Universitätsmedizin Berlin, 2008. OrthoLoad. Retrieved from <http://www.OrthoLoad.com>.

Chan, S.C.W., Walser, J., Käppeli, P., Shamsollahi, M.J., Ferguson, S.J., Gantenbein-Ritter, B., 2013. Region Specific Response of Intervertebral Disc Cells to Complex Dynamic Loading: An Organ Culture Study Using a Dynamic Torsion-Compression Bioreactor. *PLoS One* 8, e72489.

Costi, J.J., Stokes, I.A., Gardner-Morse, M.G., Iatridis, J.C., 2008. Frequency-Dependent Behavior of the Intervertebral Disc in Response to Each of Six Degree of Freedom Dynamic Loading Solid Phase and Fluid Phase Contributions. *Spine* 33, 1731–1738.

Costi, J.J., Ledet, E.H., O’Connell, G.D., 2021. Spine biomechanical testing methodologies: The controversy of consensus vs scientific evidence. *JOR Spine* 4, e1138.

Delp, S.L., Anderson, F.C., Arnold, A.S., Loan, P., Habib, A., John, C.T., Guendelman, E., Thelen, D.G., 2007. OpenSim: Open-source software to create and analyze dynamic simulations of movement. *I.E.E.E. Trans. Biomed. Eng.* 54, 1940–1950. <https://doi.org/10.1109/TBME.2007.901024>.

Fujii, R., Sakaura, H., Mukai, Y., Hosono, N., Ishii, T., Iwasaki, M., Yoshikawa, H., Sugamoto, K., 2007. Kinematics of the lumbar spine in trunk rotation: In vivo three-dimensional analysis using magnetic resonance imaging. *Eur. Spine J.* 16, 1867–1874. <https://doi.org/10.1007/s00586-007-0373-3>.

- Gawri, R., Moir, J., Ouellet, J., Beckman, L., Steffen, T., Roughley, P., Haglund, L., 2014. Physiological loading can restore the proteoglycan content in a model of early IVD degeneration. *PLoS One* 9, e101233.
- Haglund, L., Moir, J., Beckman, L., Mulligan, K.R., Jim, B., Ouellet, J.A., Roughley, P., Steffen, T., 2011. Development of a bioreactor for axially loaded intervertebral disc organ culture. *Tissue Eng. Part C Methods* 17, 1011–1019. <https://doi.org/10.1089/ten.tec.2011.0025>.
- Hartman, R.A., Yurube, T., Ngo, K., Merzlake, N.E., Debski, R.E., Brown, B.N., Kang, J.D., Sowa, G.A., 2015. Biological responses to flexion/extension in spinal segments *ex vivo*. *J. Orthop. Res.* 33, 1255–1264. <https://doi.org/10.1002/jor.22900>.
- Holsgrove, T.P., Gill, H.S., Miles, A.W., Gheduzzi, S., 2015. The dynamic, six-axis stiffness matrix testing of porcine spinal specimens. *Spine Journal* 15, 176–184. <https://doi.org/10.1016/j.spinee.2014.09.001>.
- Holsgrove, T.P., Miles, A.W., Gheduzzi, S., 2017. The application of physiological loading using a dynamic, multi-axis spine simulator. *Med. Eng. Phys.* 41, 74–80. <https://doi.org/10.1016/j.medengphy.2016.12.004>.
- Holsgrove, T.P., Amin, D.B., Pascual, S.R., Ding, B., Welch, W.C., Gheduzzi, S., Miles, A.W., Winkelstein, B.A., Costi, J.J., 2018. The equivalence of multi-axis spine systems: Recommended stiffness limits using a standardized testing protocol. *J. Biomech.* 70, 59–66. <https://doi.org/10.1016/j.jbiomech.2017.09.010>.
- Illien-Jünger, S., Gantenbein-Ritter, B., Grad, S., Lezuo, P., Ing, D., Ferguson, S.J., Alini, M., Ito, K., 2010. The Combined Effects of Limited Nutrition and High-Frequency Loading on Intervertebral Discs With Endplates. *Spine (Phila Pa 1976)* 35, 1744–1752.
- Lazaro-Pacheco D, Holsgrove TP, 2023. Load Informed Kinematic Evaluation (LIKE) protocols for the simulation of daily activities in the intervertebral disc (IVD), in: 4th International Workshop on Spine Loading and Deformation. Berlin.
- Lotz, J.C., Chin, J.R., 2000. Intervertebral Disc Cell Death Is Dependent on the Magnitude and Duration of Spinal Loading. *Spine (Phila Pa 1976)* 25, 1477–1483.
- Lund, M. E., de Zee, M., & Rasmussen, J., 2011. Comparing calculated and measured curves in validation of musculoskeletal models, in: XIII International Symposium on Computer Simulation in Biomechanics.
- Paul, C.P.L., Zuiderbaan, H.A., Zandieh Doulabi, B., van der Veen, A.J., van de Ven, P.M., Smit, T.H., Helder, M.N., van Royen, B.J., Mullender, M.G., 2012. Simulated-physiological loading conditions preserve biological and mechanical properties of caprine lumbar intervertebral discs in *EX vivo* culture. *PLoS One* 7, e33147.
- Rohlmann, A., Graichen, F., Bender, A., Kayser, R., Bergmann, G., 2008. Loads on a telemeterized vertebral body replacement measured in three patients within the first postoperative month. *Clin. Biomech.* 23, 147–158. <https://doi.org/10.1016/j.clinbiomech.2007.09.011>.
- Schultz, A., Andersson, G., D4, M., Ortengren, R., Haderspecht, K., Nachemson, A., 1982. Loads on the Lumbar Spine - Validation of a biomechanical analysis by measurements of intradiscal pressures and myoelectric signals. *J. Bone Joint Surg.* 64-A, 713–720.
- SENIAM - Recommendations for sensor locations in trunk or (lower) back muscles, 2022.
- Senteler, M., Weisse, B., Rothenfluh, D.A., Snedeker, J.G., 2016. Intervertebral reaction force prediction using an enhanced assembly of OpenSim models. *Comput. Methods Biomech. Biomed. Eng.* 19, 538–548. <https://doi.org/10.1080/10255842.2015.1043906>.
- Seth, A., Hicks, J.L., Uchida, T.K., Habib, A., Dembia, C.L., Dunne, J.J., Ong, C.F., DeMers, M.S., Rajagopal, A., Millard, M., Hamner, S.R., Arnold, E.M., Yong, J.R., Lakshminanth, S.K., Sherman, M.A., Ku, J.P., Delp, S.L., 2018. OpenSim: Simulating musculoskeletal dynamics and neuromuscular control to study human and animal movement. *PLoS Comput. Biol.* 14, e1006223.
- Stokes, I.A.F., Gardner-Morse, M., 2003. Spinal stiffness increases with axial load: Another stabilizing consequence of muscle action. *J. Electromyogr. Kinesiol.* 13, 397–402. [https://doi.org/10.1016/S1050-6411\(03\)00046-4](https://doi.org/10.1016/S1050-6411(03)00046-4).
- Takahashi, I., Kikuchi, S., Sato, K., Sato, N., 2006. Mechanical Load of the Lumbar Spine During Forward Bending Motion of the Trunk - A Biomechanical Study. *Spine (Phila Pa 1976)* 31, 18–23.
- Walter, B.A., Korecki, C.L., Purmessur, D., Roughley, P.J., Michalek, A.J., Iatridis, J.C., 2011. Complex loading affects intervertebral disc mechanics and biology. *Osteoarthritis Cartilage* 19, 1011–1018. <https://doi.org/10.1016/j.joca.2011.04.005>.
- Wilke, H.-J., Neef, P., Hinz, B., Seidel, H., Claes, L., 2001. Intradiscal pressure together with anthropometric data \pm a data set for the validation of models. *Clin. Biomech.* 16, 111–126.